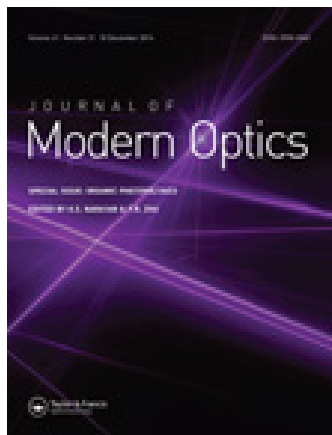


This article was downloaded by: [Bilkent University]

On: 17 December 2014, At: 23:40

Publisher: Taylor & Francis

Informa Ltd Registered in England and Wales Registered Number: 1072954 Registered office: Mortimer House, 37-41 Mortimer Street, London W1T 3JH, UK



Journal of Modern Optics

Publication details, including instructions for authors and subscription information:

<http://www.tandfonline.com/loi/tmop20>

An improved polymer solar cell incorporating single-wall carbon nanotubes

Fen Lu^a, Dewei Zhao^b, Junling Song^a, Jing Chen^c, Swee Tiam Tan^b, Lin Ke^d, Hilmi Volkan Demir^{ab}, Handong Sun^a & Xiao Wei Sun^b

^a Division of Physics and Applied Physics, School of Physical & Mathematical Sciences, Nanyang Technological University, Singapore, Singapore

^b School of Electrical and Electronic Engineering, Nanyang Technological University, Singapore, Singapore

^c School of Electronic Science and Engineering, Southeast University, Nanjing, China

^d Institute of Materials Research and Engineering, A*STAR (Agency for Science, Technology and Research), Singapore, Singapore

Published online: 17 Oct 2014.



[Click for updates](#)

To cite this article: Fen Lu, Dewei Zhao, Junling Song, Jing Chen, Swee Tiam Tan, Lin Ke, Hilmi Volkan Demir, Handong Sun & Xiao Wei Sun (2014) An improved polymer solar cell incorporating single-wall carbon nanotubes, *Journal of Modern Optics*, 61:21, 1761-1766, DOI: [10.1080/09500340.2014.971080](https://doi.org/10.1080/09500340.2014.971080)

To link to this article: <http://dx.doi.org/10.1080/09500340.2014.971080>

PLEASE SCROLL DOWN FOR ARTICLE

Taylor & Francis makes every effort to ensure the accuracy of all the information (the "Content") contained in the publications on our platform. However, Taylor & Francis, our agents, and our licensors make no representations or warranties whatsoever as to the accuracy, completeness, or suitability for any purpose of the Content. Any opinions and views expressed in this publication are the opinions and views of the authors, and are not the views of or endorsed by Taylor & Francis. The accuracy of the Content should not be relied upon and should be independently verified with primary sources of information. Taylor and Francis shall not be liable for any losses, actions, claims, proceedings, demands, costs, expenses, damages, and other liabilities whatsoever or howsoever caused arising directly or indirectly in connection with, in relation to or arising out of the use of the Content.

This article may be used for research, teaching, and private study purposes. Any substantial or systematic reproduction, redistribution, reselling, loan, sub-licensing, systematic supply, or distribution in any form to anyone is expressly forbidden. Terms & Conditions of access and use can be found at <http://www.tandfonline.com/page/terms-and-conditions>

An improved polymer solar cell incorporating single-wall carbon nanotubes

Fen Lu^a, Dewei Zhao^b, Junling Song^a, Jing Chen^c, Swee Tiam Tan^b, Lin Ke^d, Hilmi Volkan Demir^{a,b}, Handong Sun^a and Xiao Wei Sun^{b*}

^aDivision of Physics and Applied Physics, School of Physical & Mathematical Sciences, Nanyang Technological University, Singapore, Singapore; ^bSchool of Electrical and Electronic Engineering, Nanyang Technological University, Singapore, Singapore; ^cSchool of Electronic Science and Engineering, Southeast University, Nanjing, China; ^dInstitute of Materials Research and Engineering, A*STAR (Agency for Science, Technology and Research), Singapore, Singapore

(Received 13 March 2014; accepted 25 September 2014)

We present an improved efficiency of polymer solar cell by incorporating single-wall carbon nanotubes (SWCNTs). A power conversion efficiency of 2.66% was achieved for the device with 0.125 wt% SWCNTs, which is 16% improvement over control device without SWCNTs, primarily due to the increase in the photocurrent and fill factor. The results reveal that SWCNTs serve as effective and additional electron pathways, facilitating the electron transport and improving the interface contact between active layer and electrode. The improved contact area was evidenced by the increased root-mean-square surface roughness as SWCNTs concentration increases. However, the increased peak-to-valley value also indicates the possibility of short circuit in device, thus the concentration of SWCNTs has to be optimized.

Keywords: Single-wall carbon nanotube; efficiency improvement; polymer solar cell

1. Introduction

Polymer solar cells (PSCs) have been investigated intensively due to their advantages in the solution process, flexible substrates, low cost fabrication, etc. The dramatic developments in the past few years make it promising for commercial application [1–14]. The operation of PSCs mainly includes the following steps: (1) light absorption by the photoactive layers, i.e. donor and acceptor; (2) excitons (electron–hole pairs) formation in organic photoactive layer; (3) exciton diffusion and dissociation, where the exciton dissociation occurs only at donor/acceptor interface via an ultrafast charge transfer between the lowest unoccupied molecular orbits of donors and acceptors; (4) charge transport, i.e. the electrons and holes transport through their individual percolating pathways; and (5) charge collection, i.e. these charges are extracted by the corresponding electrodes. Thus, the device performance can be improved by enhancing the efficiency in each step. However, the power conversion efficiency (PCE) of PSCs is limited by the short exciton diffusion length and small charge carrier mobility of organic semiconductors. In order to overcome the limitation of exciton diffusion length and increase in the exciton diffusion/dissociation efficiency, bulk heterojunction (BHJ) blend of donors and acceptors is generally used. Furthermore, the formation of the nanoscale morphology facilitates charge transport in the interpenetrating networks [8,15–17]. Although thick photoactive layer essentially absorbs more photons, the small

charge mobility suppresses the charge transport in thick photoactive layer. Presently, 1-(3-methoxycarbonyl)-propyl-1-phenyl-(6,6)C₆₁ (PCBM) is widely used as the electron acceptor for the exciton separation and provide the percolated pathway for electron transport, however, the large volume of PCBM limits the light absorption of donor photoactive layer such as poly(3-hexylthiophene) (P3HT) and Poly[2-methoxy-5-(3,7-dimethyloctyloxy)-1,4-phenylene-vinylene] (MDMO-PPV). Some researchers have demonstrated ~25% efficiency enhancement on P3HT/PCBM devices performance through near infrared region (NIR) sensitization using small bandgap polymers [18,19]. Another method is to incorporate nanostructure semiconductors with high charge mobility, providing additional percolated pathway for efficient charge transport [20,21]. Except for high charge mobility, the energy levels of semiconductors and PCBM should be matched to facilitate the charge transfer and transport.

Carbon nanotubes (CNTs) are considered as an excellent medium for electron transport and a promising candidate for indium tin oxide (ITO) electrode replacement due to their superior electron transport property and proper work function [22–24]. In particular, functionalized single-wall carbon nanotubes (SWCNTs) have been a good choice for application in PSCs [25–28]. SWCNTs have been firstly reported that they could be mixed with donor polymer poly(3-octylthiophene) (P3OT) to provide exciton separation sites between P3OT and CNTs, as well as efficient electron transport through SWCNTs, resulting

*Corresponding author. Email: exwsun@ntu.edu.sg

in improved photocurrent generation in such blend-based PSCs [29]. Then, SWCNTs were introduced into other blends of polymer BHJ-based PSCs to enhance the electron transport [27]. It is worth mentioning that the introduction of SWCNTs in the polymer facilitates the charge transport and increases the photocurrent, however, the increase in the concentration of SWCNTs can also induce the short-circuit effects due to the comparable length of SWCNTs with the thickness of the photoactive layer [25,27]. Therefore, the concentration of SWCNTs in the polymer blend has to be optimized in order to obtain desired function of enhancing exciton separation and charge transport in such blend films.

This paper presents a simple universally applicable method to improve PSCs performance by incorporating SWCNTs in P3HT:PCBM blend. The SWCNTs were used after simple purification without other treatments. The device was optimized at much lower SWCNTs concentration of 0.125 wt% (weight ratio), which was effective to the optical properties of the active layer and cost effective, compared to the reported concentration range 0.2–1.0 wt% [25–29]. The PCE of SWCNTs-based PSCs reaches 2.66% due to the increase in short-circuit current density (J_{sc}) and fill factor (FF), which represents approximately 16% improvement over the control device without SWCNTs. The results confirm that SWCNTs serve as an efficient electron pathway, facilitating the electron transport. However, with the increase in SWCNTs concentration, the morphology of the active layers changes significantly, as characterized by atomic force microscopy (AFM), thus the concentration was optimized to increase the contact between the active layer and the electrode to avoid short circuit in devices.

2. Experimental methods

SWCNTs used in this study were from Sinopharm Chemical Reagent Co. Ltd. P3HT and PCBM from Rieke Metals Inc. and Nano-C, respectively. The SWCNTs as received were hydrothermally treated to remove catalyst residue and impurities as reported [27,28,30]. The purified SWCNTs was dissolved in chlorobenzene and sonicated at 60 °C for 1 h. Then, different volumes of SWCNTs solution were blended into P3HT:PCBM solution, followed by stirring overnight.

All devices were fabricated on ITO coated glass (20 Ω /square). The substrates were cleaned in an ultrasonic bath with detergent, deionied-water, acetone, and isopropyl alcohol successively for 15 min. After being dried in a laboratory oven, the ITO surfaces were treated by oxygen plasma for 5 min. Poly(3,4-ethylenedioxythiophene): poly(styrenesulfonate) (PEDOT:PSS) (Baytron P 4083) with a thickness of 40 nm was firstly spin-coated onto ITO-glass, and baked at 125 °C for 30 min. Subsequently, the substrates were moved into a glove

box filled with N₂ (H₂O < 0.1 ppm and O₂ < 0.1 ppm). The polymer active layers made of P3HT and PCBM (1:0.8 wt) in chlorobenzene (18 mg/mL) blended with 0, 0.125, and 0.25 wt% SWCNTs were spin-coated onto PEDOT:PSS coated substrates, respectively, and heated on a hot plate at 80 °C for 20 min in order to evaporate the remaining solvent. The thickness of the active layer before and after incorporating SWCNTs is around 200 nm. Then, the substrates were put into the metal deposition chamber (9.0×10^{-5} Pa) for E-beam evaporation of Al. All devices were post-annealed at 160 °C for 10 min with an active area of 0.1 cm².

The optical absorption spectra were recorded using UV–vis–NIR scanning spectrophotometer (UV-3101PC). The current–voltage (I – V) characteristics were measured with a Keithley 2400 sourcemeter in dark and under 100 mW/cm² (AM 1.5G) irradiation from a solar simulator (Solar Light Company Inc.). The film thickness was measured with a surface profiler (Tencor P15). Tapping mode AFM (D5000 Veeco) was used to characterize the surface topography (height image) of the active layers prepared by spin-coating polymer solution onto PEDOT:PSS coated ITO glass. Transmission electron microscopy (TEM) image was taken using JEM-1400 (JEOL). The incident photon-to-electron conversion efficiencies (IPCEs) were measured using customer designed external quantum efficiency (EQE) system comprising of 200 W Xenon lamp light source (Newport) and monochromator (Cornerstone, 130 1/8 m). The power density is precalibrated against silicon reference cell. The device structure with SWCNTs incorporated and energy level diagram of the device are shown in Figure 1.

3. Results and discussions

Figure 2 shows the TEM image of SWCNTs, exhibiting the SWCNTs' diameter of around 10 nm. Scanning electron microscopy was also tried to capture cross section images, but due to the equipment limitation and the very thin film, no significant feature was resolved. It has to be pointed out that SWCNTs should be randomly distributed in the blend layer since no orientation alignment was done in the solution preparation and spin-coating processes. Fine dispersion of SWCNTs in the blend results in the increased conductivity. The SWCNTs work as efficient pathways for electron transport due to the freeway-like network resulted high electron mobility [22], which reduces the possibility of charge recombination at the donor and acceptor interface.

Figure 3(a) shows the optical absorption spectra of the active layers with different concentration of SWCNTs. It is evident that all active layers exhibit the characteristic spectrum of P3HT:PCBM blend. The large enhancement of light absorption was observed at wavelength near 400 and 600 nm. However, the active layer

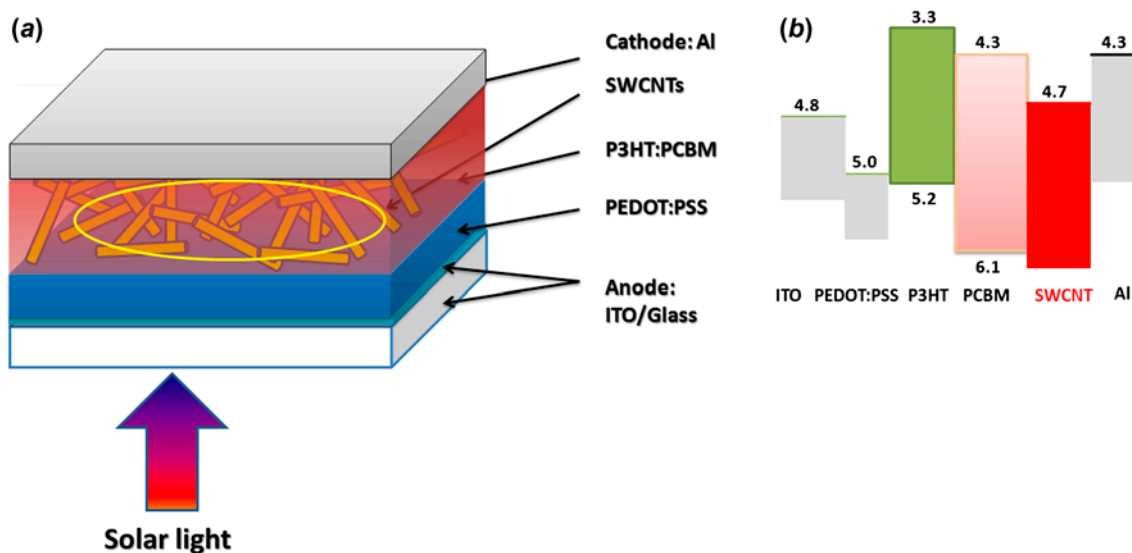


Figure 1. (a) The device structure of SWCNTs-based PSCs. (b) The energy level diagram of SWCNTs-based PSCs in eV. (The colour version of this figure is included in the online version of the journal.)

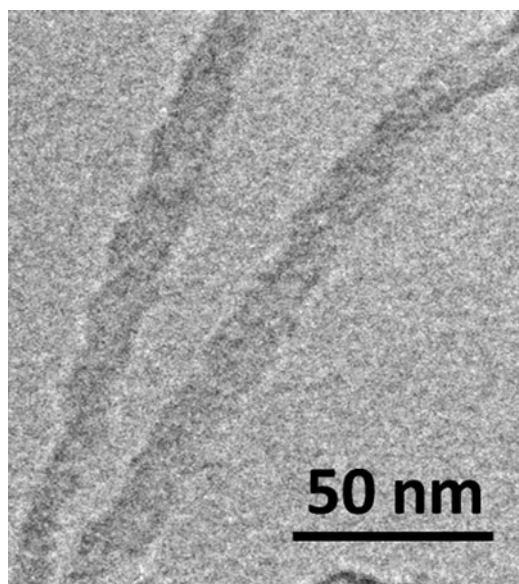


Figure 2. The TEM image of the SWCNTs, exhibiting a diameter of around 10 nm.

with 0.25 wt% SWCNTs reflects a slight change of spectrum shape, likely due to the excess incorporation of SWCNTs [24].

Figure 3(b) compares the I - V characteristics of the PSCs with different concentration of SWCNTs under simulated solar irradiation of 100 mW/cm^2 . Their corresponding performance is summarized in Table 1. In the absence of SWCNTs, the control device has a PCE of 2.28% with a $J_{\text{sc}} = 7.52 \text{ mA/cm}^2$, $V_{\text{oc}} = 0.67 \text{ V}$, and

$\text{FF} = 45.3\%$. With an incorporation of 0.125 wt% SWCNTs, the J_{sc} increases to 7.93 mA/cm^2 and FF to 51.6%, leading to the enhancement of PCE to 2.66%. However, when the concentration of SWCNTs is further increased to 0.250 wt%, the PCE reduces to 2.46%, accompanied with slightly decreased J_{sc} and FF. The improvement of PCE mainly originates from the increase in both J_{sc} and FF. Therefore, it can be concluded that the improved photocurrent density benefits from the enhancement of the charge transport due to the incorporation of SWCNTs, as evidenced by the increased FF by 14% from 45.3 to 51.6%, indicating that the SWCNTs act as the percolated path for efficient electron transport. Moreover, the incorporated SWCNTs also provide more interfacial areas for the exciton dissociation, benefiting the increase in the photocurrent [26]. Subsequently, the dissociated electrons can transport through both PCBM phase and SWCNTs, followed by the extraction by the Al cathode, as the energy level diagram shown in Figure 1 (b). However, with further increase in SWCNTs concentration, the electrical short circuits are easily formed due to the longer length of CNTs than the thickness of active layer [27], resulting in the reduced photocurrent density (7.69 mA/cm^2) and FF (50.8%). Furthermore, the inset in Figure 3 shows the I - V characteristics of PSCs with different concentrations of SWCNTs in dark. It is obvious that all devices exhibit typical diode behavior in dark. The current density in the devices with SWCNTs is increased, higher than that in the control device without SWCNTs, implying the enhancement of the charge transport by using the incorporation of SWCNTs.

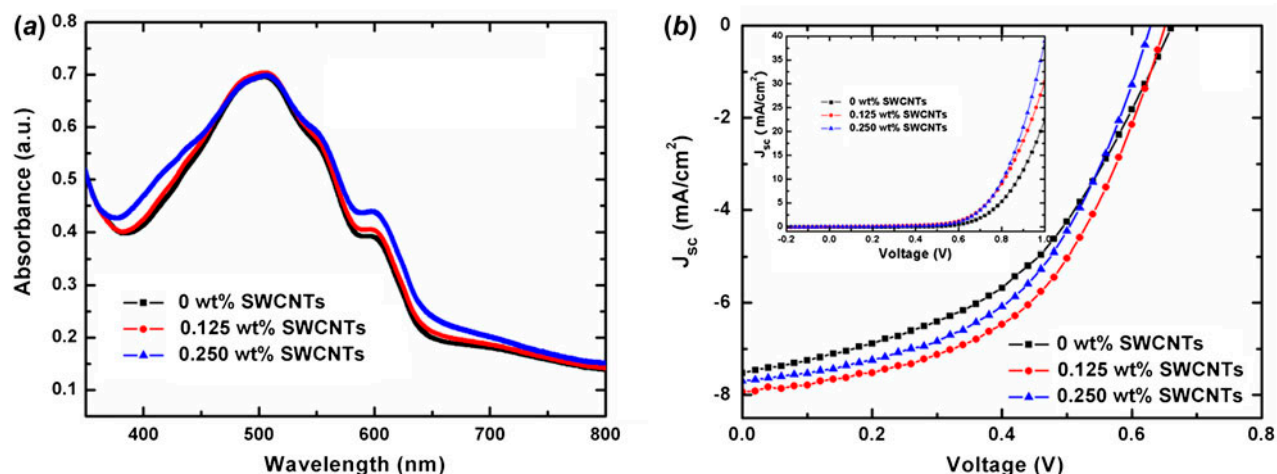


Figure 3. (a) The optical absorption spectra of the active layers with different concentration. (b) The I - V characteristics of the PSCs blended with different concentrations of SWCNTs (0, 0.125, and 0.250 wt%) under 100 mW/cm^2 . The inset shows the I - V characteristics of the corresponding PSCs in dark. All devices were annealed at 160°C for 10 min. (The colour version of this figure is included in the online version of the journal.)

Table 1. The summary of the average performance of PSCs with different concentrations of SWCNTs (weight ratio: 0, 0.125, 0.250 wt%) under 100 mW/cm^2 .

Devices (wt%)	V_{oc} (V)	J_{sc} (mA/cm^2)	FF (%)	PCE (%)
0	0.67	7.52	45.3	2.28
0.125	0.65	7.93	51.6	2.66
0.250	0.63	7.69	50.8	2.46

On the other hand, it can be seen that the V_{oc} decreases slightly with the increase in the SWCNTs concentration, which is likely caused by the short-circuit points across the active layer due to the long length of SWCNTs [27].

Figure 4 shows the tapping mode AFM height images of the active layers with different concentrations of SWCNTs. The root-mean-square surface roughness increases as the concentration of SWCNTs increases, exhibiting 0.781, 0.906, and 1.194 nm, respectively, for 0, 0.125, and 0.250 wt% active layers. The high surface roughness increases the contact area between active layer and Al cathode, beneficial to the electron extraction. However, as the SWCNTs concentration increases, the large difference of peak-to-valley (Rmax) surface roughness from 10.574, 20.900, to 24.141 nm mean a higher probability of CNT protrusion that causes electrical short circuits. Therefore, a proper concentration of incorporated SWCNTs is required for the improvement of the efficiency.

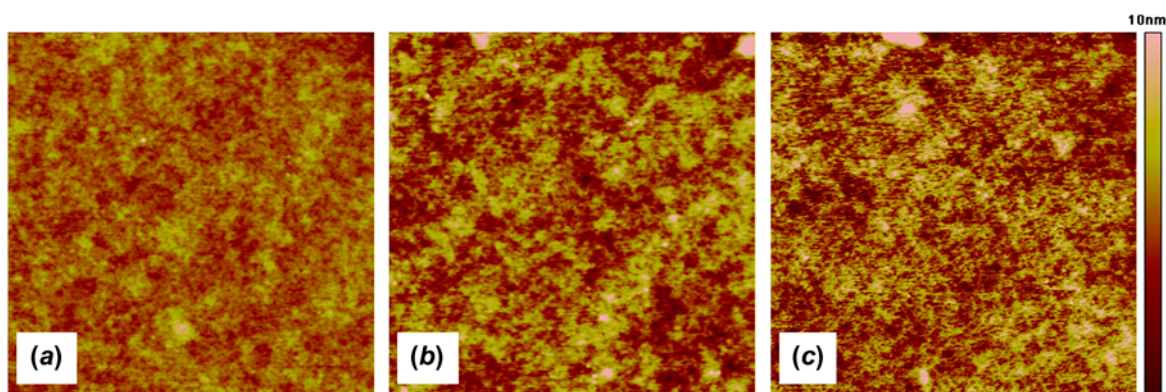


Figure 4. The tapping mode AFM height images on the surfaces of the active layers with different concentration of SWCNTs. (a) 0 wt% SWCNTs; (b) 0.125 wt% SWCNTs; (c) 0.25 wt% SWCNTs. For all images, the scan size is $5 \times 5 \mu\text{m}^2$, and the height-scale is 10 nm. All films were made on the PEDOT:PSS coated ITO substrates and annealed at 160°C for 10 min. (The colour version of this figure is included in the online version of the journal.)

Moreover, the FF is correlated with the series resistance of the device. The series resistance originates from the bulk resistance of the materials used, the electrodes resistance, and contact resistance at the interface between electrodes and active layers [31]. Herein, the series resistance of the control device without SWCNTs is $29.3 \Omega \text{ cm}^2$, larger than those of the devices with 0.125 wt% ($21.2 \Omega \text{ cm}^2$) and 0.250 wt% ($21.5 \Omega \text{ cm}^2$) SWCNTs. The slightly higher resistance at higher SWCNTs concentration could be attributed to the larger contact resistance associated with the voids and defects produced in electrode deposition on larger roughness surface. The reduced series resistance led to the improvement of FF from 45.3% to 51.6% and 50.8%, respectively. The results imply that the low FF for the control device without SWCNTs is caused by high charge recombination in the thick active layer, meanwhile, the SWCNTs incorporated provides effective and transport path for electron transport, resulting in the reduction of charge recombination [31]. On the other hand, a certain SWCNTs incorporated is beneficial to the surface contact between active layer and Al electrode, as well as to the improvement of the bulk resistance of active layer, as evidenced by the improved dark current of the devices with SWCNTs.

The IPCE spectra of fabricated devices is normalized respect to the maximum value of measured IPCE of 0.125 wt% SWCNTs device at wavelength 515 nm, as shown in Figure 5, reflecting the improved capability of converting incident photons to electrons by the incorporation of SWCNTs over the entire range of the effective spectral response due to the enhanced charge transport. The incorporation of 0.125 wt% SWCNTs provides additional pathways for electrons, which also improves the electron mobility inside the active layer and achieves the balance of charge carrier transport and extraction for

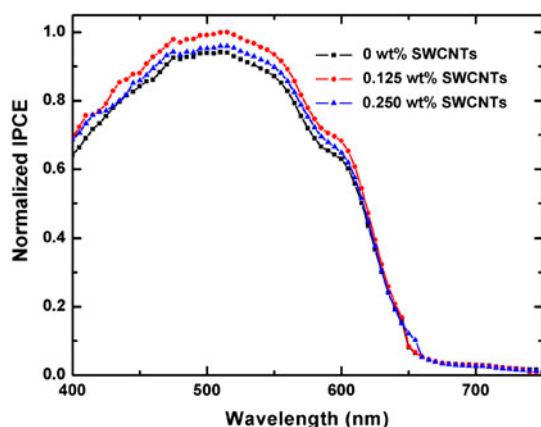


Figure 5. The normalized IPCE spectra of fabricated PSCs with different concentration of SWCNTs. (The colour version of this figure is included in the online version of the journal.)

electrons and holes. Therefore, the entire IPCE is enhanced over the whole absorption range of P3HT. However, further increase in the concentration of SWCNT to 0.25 wt% breaks the balance, leading to reductions of both short-circuit current and open-circuit voltage compared to the device with 0.125 wt% SWCNTs.

4. Conclusion

Improved performance of PSCs with SWCNTs incorporated has been presented. The results indicate that the SWCNTs can act as the effective pathway for electron transport and increase charge transport efficiency as evidenced by the improvement in both FF and J_{sc} . Surface morphology of these active layers reveals the dispersion of the SWCNTs in polymer blend, exhibiting an increased surface roughness with the increase in SWCNTs concentration.

Acknowledgements

This work was supported by New Initiative Fund and Joint Singapore-German Research Projects from Nanyang Technological University.

References

- [1] Tang, C.W. *Appl. Phys. Lett.* **1986**, *48*, 183.
- [2] Yu, G.; Gao, J.; Hummelen, J.C.; Wudl, F.; Heeger, A.J. *Science* **1995**, *270*, 1789–1791.
- [3] Reyes-Reyes, M.; Kim, K.; Carroll, D.L. *Appl. Phys. Lett.* **2005**, *87*, 083506.
- [4] Clarke, T.M.; Durrant, J.R. *Chem. Rev.* **2010**, *110*, 6736–6767.
- [5] Xie, F.-X.; Choy, W.C.H.; Wang, C.C.D.; Sha, W.E.I.; Fung, D.D.S. *Appl. Phys. Lett.* **2011**, *99*, 153304.
- [6] Zhang, M.; Gu, Y.; Guo, X.; Liu, F.; Zhang, S.; Huo, L.; Russell, T.P.; Hou, J. *Adv. Mater.* **2013**, *25*, 4944–4949.
- [7] Dou, L.; Gao, J.; Richard, E.; You, J.; Chen, C.C.; Cha, K.C.; He, Y.; Li, G.; Yang, Y. *J. Am. Chem. Soc.* **2012**, *134*, 10071–10079.
- [8] Zhao, D.; Tang, W.; Ke, L.; Tan, S.T.; Sun, X.W. *ACS Appl. Mater. Interfaces* **2010**, *2*, 829–837.
- [9] Li, X.; Choy, W.C.H.; Lu, H.; Sha, W.E.I.; Ho, A.H.P. *Adv. Funct. Mater.* **2013**, *23*, 2728–2735.
- [10] Krebs, F.C.; Gevorgyan, S.A.; Alstrup, J. *J. Mater. Chem.* **2009**, *19*, 5442.
- [11] Sun, X.W.; Zhao, D.W.; Ke, L.; Kyaw, A.K.K.; Lo, G.Q.; Kwong, D.L. *Appl. Phys. Lett.* **2010**, *97*, 053303.
- [12] Zhang, F.; Sun, F.; Shi, Y.; Zhuo, Z.; Lu, L.; Zhao, D.; Xu, Z.; Wang, Y. *Energy Fuels* **2010**, *24*, 3739–3742.
- [13] Zhang, F.J.; Zhao, D.W.; Zhuo, Z.L.; Wang, H.; Xu, Z.; Wang, Y.S. *Sol. Energy Mater. Sol. Cells* **2010**, *94*, 2416–2421.
- [14] Zhao, D.W.; Ke, L.; Li, Y.; Tan, S.T.; Kyaw, A.K.K.; Demir, H.V.; Sun, X.W.; Carroll, D.L.; Lo, G.Q.; Kwong, D.L. *Sol. Energy Mater. Sol. Cells* **2011**, *95*, 921–926.
- [15] Chirvase, D.; Parisi, J.; Hummelen, J.C.; Dyakonov, V. *Nanotechnology* **2004**, *15*, 1317–1323.
- [16] Hoppe, H.; Sariciftci, N.S. *J. Mater. Chem.* **2006**, *16*, 45.

- [17] Hoppe, H.; Niggemann, M.; Winder, C.; Kraut, J.; Hiesgen, R.; Hinsch, A.; Meissner, D.; Sariciftci, N.S. *Adv. Funct. Mater.* **2004**, *14*, 1005–1011.
- [18] Ameri, T.; Min, J.; Li, N.; Machui, F.; Baran, D.; Forster, M.; Schottler, K.J.; Dolfen, D.; Scherf, U.; Brabec, C.J. *Adv. Energy Mater.* **2012**, *2*, 1198–1202.
- [19] An, Q.; Zhang, F.; Zhang, J.; Tang, W.; Wang, Z.; Li, L.; Xu, Z.; Teng, F.; Wang, Y. *Sol. Energy Mater. Sol. Cells* **2013**, *118*, 30–35.
- [20] Beck, W.J.E.; Wienk, M.M.; Janssen, R.A. *J. Adv. Mater.* **2004**, *16*, 1009–1013.
- [21] Takanezawa, K.; Tajima, K.; Hashimoto, K. *Appl. Phys. Lett.* **2008**, *93*, 063308.
- [22] Gruner, G. *J. Mater. Chem.* **2006**, *16*, 3533.
- [23] Kymakis, E.; Amaratunga, G.A.J. *Appl. Phys. Lett.* **2002**, *80*, 112.
- [24] Wu, M.-C.; Lin, Y.-Y.; Chen, S.; Liao, H.-C.; Wu, Y.-J.; Chen, C.-W.; Chen, Y.-F.; Su, W.-F. *Chem. Phys. Lett.* **2009**, *468*, 64–68.
- [25] Berson, S.; de Bettignies, R.; Bailly, S.; Guillerez, S.; Jusselme, B. *Adv. Funct. Mater.* **2007**, *17*, 3363–3370.
- [26] Geng, J.; Zeng, T. *J. Am. Chem. Soc.* **2006**, *128*, 16827–16833.
- [27] Kymakis, E.; Kornilios, N.; Koudoumas, E. *J. Phys. D: Appl. Phys.* **2008**, *41*, 165110.
- [28] Li, C.; Chen, Y.; Wang, Y.; Iqbal, Z.; Chhowalla, M.; Mitra, S. *J. Mater. Chem.* **2007**, *17*, 2406.
- [29] Kymakis, E.; Alexandrou, I.; Amaratunga, G.A.J. *J. Appl. Phys.* **2003**, *93*, 1764.
- [30] Bahr, J.L.; Tour, J.M. *Chem. Mater.* **2001**, *13*, 3823–3824.
- [31] Moliton, A.; Nunzi, J.-M. *Polym. Int.* **2006**, *55*, 583–600.